Stem Cell Reviews and Reports (2020) 16:569–584
https://doi.org/10.1007/s12015-020-09963-y

Decellularized Cell Culture ECMs Act as Cell Differentiation Inducers

Mahmut Parmaksiz[1] · Ayşe Eser Elçin[1] · Yaşar Murat Elçin[1,2]

Published online: 13 March 2020

Abstract
Decellularized tissues and organs have aroused considerable interest for developing functional bio-scaffolds as natural templates in tissue engineering applications. More recently, the use of natural extracellular matrix (ECM) extracted from the in vitro cell cultures for cellular applications have come into question. It is well known that the microenvironment largely defines cellular properties. Thus, we have anticipated that the ECMs of the cells with different potency levels should likely possess different effects on cell cultures. To test this, we have comparatively evaluated the differentiative effects of ECMs derived from the cultures of human somatic dermal fibroblasts, human multipotent bone marrow mesenchymal stem cells, and human induced pluripotent stem cells on somatic dermal fibroblasts. Although challenges remain, the data suggest that the use of cell culture-based extracellular matrices perhaps may be considered as an alternative approach for the differentiation of even somatic cells into other cell types.

Keywords Cell culture ECM · Decellularization · Cell differentiation inducer · Tissue engineering · Regenerative biomaterials · In vitro cell culture model

Introduction

Tissue engineering (TE) is a field of regenerative medicine with emphasis on the repair/replacement of diseased or missing tissue through the in vitro use of cells and scaffolds. The main objective of TE is to develop bioconstructs which can mimic the natural in vivo three-dimensional (3D) structure of the tissues and the extracellular matrix (ECM) under laboratory conditions [1, 2]. Past studies have focused on various approaches for producing bio-scaffolds aiming to mimic the structure and function of natural ECM, albeit with limited success. There is as yet no developed bio-scaffold or tissue layer fully meeting the complex architectural structure and bio-functions of the natural ECM prepared by common physicochemical biomaterials production techniques.

Nevertheless, development of functional bio-scaffolds through the use of the biological ECM known as "decellularization" has recently aroused considerable interest. The fundamental principle behind this technique is based on the removal of cells from tissues or organs using appropriate methods, leaving a bioactive scaffold possessing the natural 3D ECM structure [3]. The essential criterion of success in decellularization is the complete removal of the cellular components, while preserving the vast majority of the active ECM content of the cells of the tissue in question [4]. Currently, decellularized ECMs originating from tissues or organs can be handled as bio-matrices for tissue engineering, as their natural 3D structure and multidirectional active composition can be preserved to a significant extent. To date, various types of tissues, including those of small intestine submucosa (SIS), cartilage, heart valves, urethra etc. have been used in preclinical TE studies with a certain level of success, and have formed the basis for the clinical use of these products [5–9]. As an alternative approach to the extraction of natural ECM from tissues or organs, ECM extraction from in vitro cell cultures have more recently drawn interest. This approach is based essentially on the collection of the natural ECM synthesized by cell cultures. Briefly, the cells of the confluent cultures are removed by standard decellularization protocols, while the ECM containing the natural bioactive molecules and proteins released by the cells is collected and used for multipurpose biomaterials or cell culture substrate

Electronic supplementary material The online version of this article (https://doi.org/10.1007/s12015-020-09963-y) contains supplementary material, which is available to authorized users.

✉ Yaşar Murat Elçin
elcin@ankara.edu.tr

[1] Tissue Engineering, Biomaterials and Nanobiotechnology Laboratory, Ankara University Faculty of Science, and Ankara University Stem Cell Institute, Ankara, Turkey

[2] Biovalda Health Technologies, Inc, Ankara, Turkey

applications [10–14]. This approach also allows to overcome some of the disadvantages of using ECMs directly from tissues/organs for TE or cell therapy applications [15, 16]. Although studies aiming to obtain the ideal cell culture ECM have reported promising results, their success remains to be limited, so the search still continues for a means of obtaining well-characterized ECMs produced in vitro that can support the in vivo functions of stem or somatic cells.

In the present study, we investigated comparative decellularization protocols for the extraction of ECM from cells with different potencies, including human somatic dermal fibroblasts (hDFs), human multipotent bone marrow mesenchymal stem cells (hBM-MSCs) and human induced pluripotent stem cells (hiPSCs) and evaluated their potential as differentiation inducers using the hDFs. After the immunophenotypical and molecular characterization of the cells were carried out, the efficacy of the decellularization protocols was compared based on spectroscopic, histologic and microscopic techniques. Bioactive contents of different types of cell culture-derived ECMs were analyzed using immunofluorescence staining, ELISA and spectroscopic methods. Later, viability, proliferation and gene expression characteristics of hDFs on all three types of ECM-covered culture plates were investigated in detail. The schematic illustration of the experimental approach is presented in Fig. 1.

Materials and Methods

Cell Cultures

hDFs (PCS-201-012), hBM-MSCs (PCS-500-012) and hiPSCs (ACS-1023) were obtained from American Type Culture Collection (ATCC, Manassas, VA). All cells were thawed in a 37 °C water bath, as per the manufacturer recommendations and transferred into respective culture media. hDFs which were isolated from 40 to 45 year-old female donors ($N = 3$) were maintained in a serum-free fibroblast growth medium (ATCC, PCS-201-040) containing 10 U/mL penicillin/10 μg/mL streptomycin (Pen/Strep) and cultured in 25 cm^2 culture plates at a density of 4,000–5,000 cells/cm^2. The medium was exchanged with fresh growth medium after 24 h, then every other day and cultured until 80% confluence was achieved. The cells were monitored by standard methods and passaged using 0.25% trypsin-EDTA solution, and replated at a ratio of 1:6. Three independent cell cultures were pooled and stocked for further studies. Cells from passages 6–10 were used in advanced characterization and decellularization studies. hBM-MSCs were plated at a density of 5,000 cells/cm^2 in MSC growth medium (ATCC, PCS-500-041) containing Pen/Strep and maintained until passages 2–5.

hiPSCs were adapted initially to the culture as per the recommendations of the manufacturer. To this end, cells were seeded onto 60 mm culture plates coated with CellMatrix™ (ATCC, ACS-3035), prepared at a concentration of 150 μg/mL in 2 mL of cold DMEM:F12. The stock cells were suspended in a Pluripotent Stem Cell SFM XF/FF growth medium containing 1 mL 10 μM ROCK inhibitor and separated onto two culture plates. After reaching ~80% confluence, the cell colonies were detached using the dissociation reagent (ATCC, ACS 3010), and the culture was maintained after splitting at 1:4 ratio. hiPSCs were then transferred into vitronectin-coated (VTN-N; 0.5 μg/cm^2) plates, and cultured in Essential 8™ Medium (Gibco, A1517001) containing Essential 8™ Supplement. hiPSCs were passaged using a 0.5 mM EDTA solution in phosphate-buffered saline (pH 7.4; PBS). All cell types were cultured in an incubator adjusted to 5% CO_2, 37 °C and > 95% humidity. The cells were monitored and photographed daily using a digital phase-contrast microscope.

Immunophenotype Characterization

A fluorescent-activated cell separation-based immunophenotypic characterization (FACS) procedure was carried out using a Beckman Coulter Navios FCM device using the following antibody panel: CD31, CD10 CD26, CD 90 and CD105 for hDFs; CD29, CD31, CD34, CD73, CD90 and CD105 for hBM-MSCs; and Oct3/4, Nanog, Sox2, SSEA-4, TRA-1-60 and TRA-1-81 for hiPSCs.

The cells were collected once they reached 80% confluence and washed with the buffer solution. Afterwards, the cells were suspended in the buffer to reach a cell density of 2.0–3.0 × 10^6 for each cell type, and centrifuged for 10 min at 250×*g*. The obtained pellet was suspended in a 1 mL buffer, and 100 μL samples were transferred to tubes for analysis, for which 5 μL of antibody solution was added, and the solution was incubated for 20 min. The samples were then suspended in the buffer solution after a series of washes and placed into the device (Beckman Coulter Navios FCM) for reading. Collected data were analyzed using Kaluza software.

Quantitative RT-Polymerase Chain Reaction

After the cells reached ~80% confluence, they were collected from the culture dishes and prepared for qRT-PCR analyses. cDNA samples from isolated total RNA were examined using the LightCycler® 96 Real-Time PCR System (Roche Life Sci., Belmont, CA), following the LightCycler® 480 Probes Master protocol. The probes of the selected target genes were obtained from Roche [17, 18] (listed in supplementary Table I). qRT-PCR reaction conditions were as follows: 10 s at 95 °C, 30 s at 60 °C and 1 s at 72 °C for 45 cycles for amplification, then 30 s 40 °C for cooling. Expression levels of the target genes were calculated using the ΔΔCt method. The experiments were performed in triplicate, and HPRT1

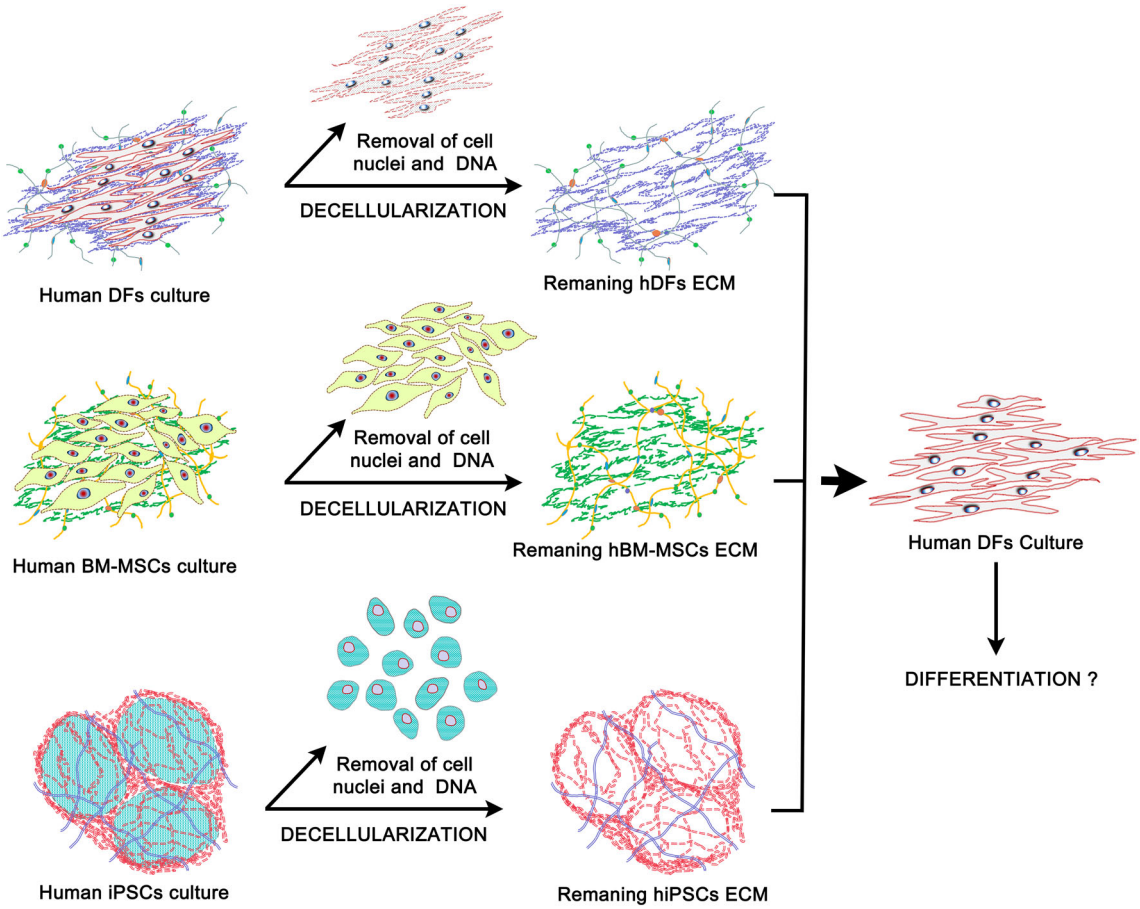

Fig. 1 Schematic illustration of the experimental approach

was used as the reference gene. The pluripotency gene expression levels of the human iPSCs were calculated by reference to the un-transfected hDF cells (iPSCs had been derived from hDFs).

Decellularization of Cell Culture

At first, all cell types were proliferated under respective culture conditions until they reached full confluence, confirmed by phase-contrast microscopy. Decellularization protocols were then applied on cell cultures. Briefly, the cultures underwent the process for the release of the nucleic acid content by degradation of the cell membrane and removal of the cells until the ECM was retained. Decellularization was monitored by phase contrast microscopy and photographed (Zeiss). Three independent protocols were investigated for optimization: In Protocol 1, the cultures were treated for 20 min with a 1% volume Triton X-100 solution in sterile distilled water (dH_2O). Repetitive washes were carried out with PBS before and after the process. In Protocol 2, the cultures were treated for 20 min with a 1% volume Triton-X-100 solution in dH_2O. In the second stage, they were washed in PBS and treated for 30 min with a 150 U/mL DNase-1 solution in PBS at 37 °C. In the final stage, a repetitive series of washes were performed with PBS. In Protocol 3, the cultures were treated for 15 min with a 20 mM NH_4OH solution prepared in a 1% Triton X-100 in PBS. In the final stage, a repetitive series of washes were done with PBS.

DNA Content Analysis

The DNA contents of the respective decellularized cultures were analyzed by the spectrophotometric method. For this purpose, the retained ECM specimens on the plate surfaces were incubated for 48 h at 55 °C with a solution comprising 10 mM Trizma, 50 mM KCl, 1.5 mM $MgCl_2$, 0.5% Tween 20 and 20 mg/mL Proteinase K. The solution was collected and centrifuged for 15 min at +4 °C and at 3000 rpm to remove the supernatant. DNA was extracted from the collected supernatant by the phenol:chloroform:isoamyl alcohol method. The extraction solution was centrifuged for 10 min at 25 °C and at 10,000 rpm, and the supernatant was discarded. The remaining pellet was mixed with 100 μL dH_2O and the DNA content was measured using Nanodrop 2000c spectrophotometer (Thermo), and the efficacy of the decellularization process was quantified based on the percentage decrease in DNA

content. For each group of ECM, the untreated hDFs, hBM-MSCs and hiPSCs were used as controls.

H&E Staining of Decellularized ECM

In addition to the DNA content analysis (presence of potential cell nuclei), retained ECM distribution in the decellularized ECMs was analyzed through histochemical evaluations. To this end, cell-culture based ECMs were washed in PBS following decellularization, and fixed in 2.5% glutaraldehyde. Following serial washing (2 min with 95% alcohol and 2 min with 70% alcohol), the samples were treated for 8 min with a hematoxylin solution, washed with water for 5 min and activated for 30 s using a 1% acid-alcohol solution. The samples were then washed again and cross-stained with eosin-B for ~1 min, after which they were dehydrated with 95% alcohol. In the final stage, the stained samples were investigated under a light microscope (Leica).

Quantification of sGAGs

The amounts of sulfated glycosaminoglycans (sGAGs) in the cell-based ECMs obtained from the decellularization procedure were determined by using the Blyscan sGAG detection kit (Biocolor, Newtonabbey, UK), following the standard protocol recommended by the manufacturer. For this purpose, cell-culture based ECMs were treated separately with a papain extraction solution and incubated in an axial mixer for 3 h at 65 °C. The lysate obtained was collected and mixed with the blyscan-stain provided in the kit, and then centrifuged for 10 min at 10,000×*g*. The supernatant was then discarded and a dissociation solution was added to the collected pellet. The sGAG amount was measured spectrophotometrically at a wavelength of 656 nm. Untreated cell cultures were considered as controls for a comparison of the decrease in sGAG amounts.

Morphological Characterization

SEM was used to investigate the efficacy of decellularization based on the distribution of the retained ECMs in the culture dishes. For this purpose, decellularized culture surfaces were washed in PBS, and fixed in glutaraldehyde (2.5%). Then they were washed again in PBS, and dehydrated through ethanol series (50–95%). After critical point drying, the samples were coated with a thin layer of gold and imaged using an Evo 10 model SEM (Zeiss, Oberkochen, Germany).

Immunofluorescence Stainings

The prospective proteins present in the cell-culture based ECMs were identified by immunofluorescence stainings. Briefly, the samples were fixed in cold methanol, then the fixed cells and cell-culture based ECMs were repetitively washed in 1 mL PBS. Following aspiration of PBS, the fixed samples were permeabilized by adding PBS containing 1% BSA for 30 min at room temperature. Then, the samples were incubated for 3 h at room temperature with the primary antibodies which were diluted 1:100 in 1% BSA buffer (listed in Supplementary Table II).

After that, the samples were washed three times in PBS containing 1% BSA, and incubated for 45 min with Alexa Fluor® 488 (10 μg/mL) in dark room to avoid bright light exposure. Finally, the stained samples were imaged using a ZEISS®ImagerZ2 (Zeiss).

Quantification of Growth Factors

After the samples were washed with PBS, a urea-heparin extraction solution was added into culture plates and kept on an orbital shaker for 24 h at +4 °C, after which, the samples were collected and transferred to tubes and centrifuged for 10 min at 12,000 rpm. The supernatant was collected after centrifugation and growth factors were analyzed. ELISA kits for VEGF (KHG0111), and TGFB-1 (BMS249–4) were obtained from ThermoFisher; PDGF-AB ELISA kit (DHD00C) was purchased from R&D Systems (Minneapolis, MN).

Seeding of hDFs on Cell ECM Surfaces

The behavior of somatic hDFs was investigated in 2D cultures covered with ECM obtained from three different cell types having different characteristics and potencies. The medium of hDF cultures (at passages 5–7) was removed once the cells reached ~80% confluence, then washed in PBS, before detaching the cells from the surface by trypsin-EDTA treatment. The cell pellet obtained after centrifugation was suspended in DMEM-F12 containing 10% FBS and 1% Pen/Strep, and the cells (~3000 cells/cm^2) were seeded onto 24-well culture plates covered with decellularized ECMs retained from either hDFs, hBM-MSCs or hiPSC cultures. The cultures were maintained in an incubator adjusted to 5% CO_2 and 37 °C. The hDFs were also seeded on standard culture plates as the control group.

Cell Viability and Proliferation Capacity of DFs on Cell Culture-Based ECMs

After the seeding of somatic hDFs on the surface of culture plates covered with different cell-based ECMs, their viability and proliferation capacity were identified at certain time points (days 1, 3 and 7) using a commercial MTT [3-(4,5-dimethylthiazol-2-yl)-2,5-diphenyltetrazolium bromide] kit, which detects changes in cellular mitochondrial dehydrogenase activity. The samples were washed after discarding the growth medium, and the MTT reagent was added at a ratio of

1/10. The growth medium was removed after 4 h of incubation in an incubator adjusted to 5% CO_2 at 37 °C, the obtained formazan was collected using a solvent and measurements were taken at a wavelength of 570 nm using a SpectraMax® M5 microplate reader (Molecular Devices, San Jose, CA).

In addition to the spectrophotometric quantitative analysis for the monitoring of cell viability, the effects of ECM-covered surfaces on the viability and proliferation of hDFs were investigated and recorded using a phase-contrast microscope.

Surface Characterization of Cell Seeded ECMs

SEM analyses were performed to monitor the adhesion and proliferation properties of hDFs on 2D-culture surfaces covered with different cell-based ECMs. Similarly, after the somatic hDFs were seeded on the culture surfaces covered with different cell-based ECMs, the samples were fixed in 2.5% glutaraldehyde prepared in PBS at certain time points (days 1, 3 and 7), washed in PBS, and dehydrated by passing the samples through a series of ethanol (50–95%). After the critical drying process, the sample surfaces were covered with a thin layer of gold and investigated under the SEM.

Identification of Gene Expression Levels of hDFs on Cell Culture-Based ECMs

The changes in the gene expression levels of hDFs under the influence of external factors found in the rich content of different ECM types were evaluated. The hDFs were seeded on different cell culture-based ECM-covered T75 culture plates and maintained under standard culture conditions. hDFs reaching ~80% confluence (within 6–7 days) were collected for the identification of the gene expression levels. The hDFs proliferated on culture plates were considered as the controls, and changes in gene expression levels were compared. BMP2, COL1A1, SOX2, POU5F1 (OCT4), KLF4, FSP1 (S1100A4), SMAD4, THY1, VWF, KAT2B (PCAF), CD106 (VCAM1), BMP6, NANOG and CD44 genes were analyzed for this purpose.

Statistical Analysis

All analyses performed in the study were independently repeated three times ($n = 3$) and the results were expressed as mean ± standard deviation values. Statistical analyses were carried out in the GraphPad Prism 7 program using a one-way ANOVA test, and significant differences were identified through Tukey's post hoc analyses. The level of significance was considered as * $p \leq 0.05$, ** $p \leq 0.01$, *** $p \leq 0.001$, **** $p \leq 0.0001$.

Results

Characterization of Cultured Cells

The cells demonstrated typical immunophenotypes and gene expressions. Three different types of commercially-obtained human cell lines were cultured and characterized using standard methods, including qRT-PCR and flow cytometry. Firstly, the typical fibroblastic cell morphology of hDFs was confirmed by phase-contrast microscopy on day 7 of passage 7 (Fig. 2a). Immunophenotype analysis revealed that the somatic hDFs were positive for the surface antigens CD10, CD26, CD105, CD90, while they lacked the surface antigen expressions of CD31, LIN and HLA DR (Fig. 2b, supplementary Fig. 1). In addition, qRT-PCR analysis revealed that hDFs have specific gene expressions [19] for FSP1, and THY1, while they expressed low levels of SMAD4, PCAF, PPAR and KLF4 (Fig. 2c).

The second cell type, hBM-MSCs used in the study adhered and proliferated well on culture plates and preserved their typical fibroblastoid fusiform morphology during culture (Fig. 2d; passage 2, day 7). In line with their characteristics [17], the multipotent hBM-MSCs expressed high levels of CD73 (98.55%), CD90 (91.67%), CD105 (99.57%) and CD29 (99.66%) antigens (Fig. 2e, supplementary Fig. 2), while not expressing CD34, LIN, CD31, HLA DR or CD133. Additionally, they expressed BMP2, BMP6, CD44, VCAM1 and vWF, which were selected from the characteristic gene panel (Fig. 2f).

The third cell type was hiPSCs, which is acquired by the reprogramming of adult somatic hDFs via the transfer of Oct3/4, Sox2, Klf4 and c-Myc genes. hiPSCs proliferated well on vitronectin (VTN)-coated culture plates, and acquired the typical colony form in ongoing passages (Fig. 2g; passage 21). Besides the cell phenotype, expression of pluripotency genes, along with the existence of certain surface markers are commonly used to identify the hiPSCs [20]. Flow cytometry findings demonstrated the presence of the surface antigens Nanog, OCT3/4, Sox2, SSEA4, TRA-1-60, TRA-1-81, while not expressing CD45 (Fig. 2h, supplementary Fig. 3). In addition, the quantitative RT-PCR analysis showed that the hiPSCs expressed Sox2, OCT3/4, Nanog and Klf4 genes (Fig. 2i).

H&E and SEM Results of Decellularized Cell-Cultures

Complete decellularization was achieved in all three types of cells. After the cells reached full confluence in each of their standard culture media, three different protocols for the retrieval of decellularized ECM from different cell types were investigated. The essential requirement of an optimal decellularization protocol is the removal of the DNA and cell nuclei from the cells, while ensuring maximum preservation of the ECM content [7, 21]. Figure 3a shows the findings of the hematoxyline &

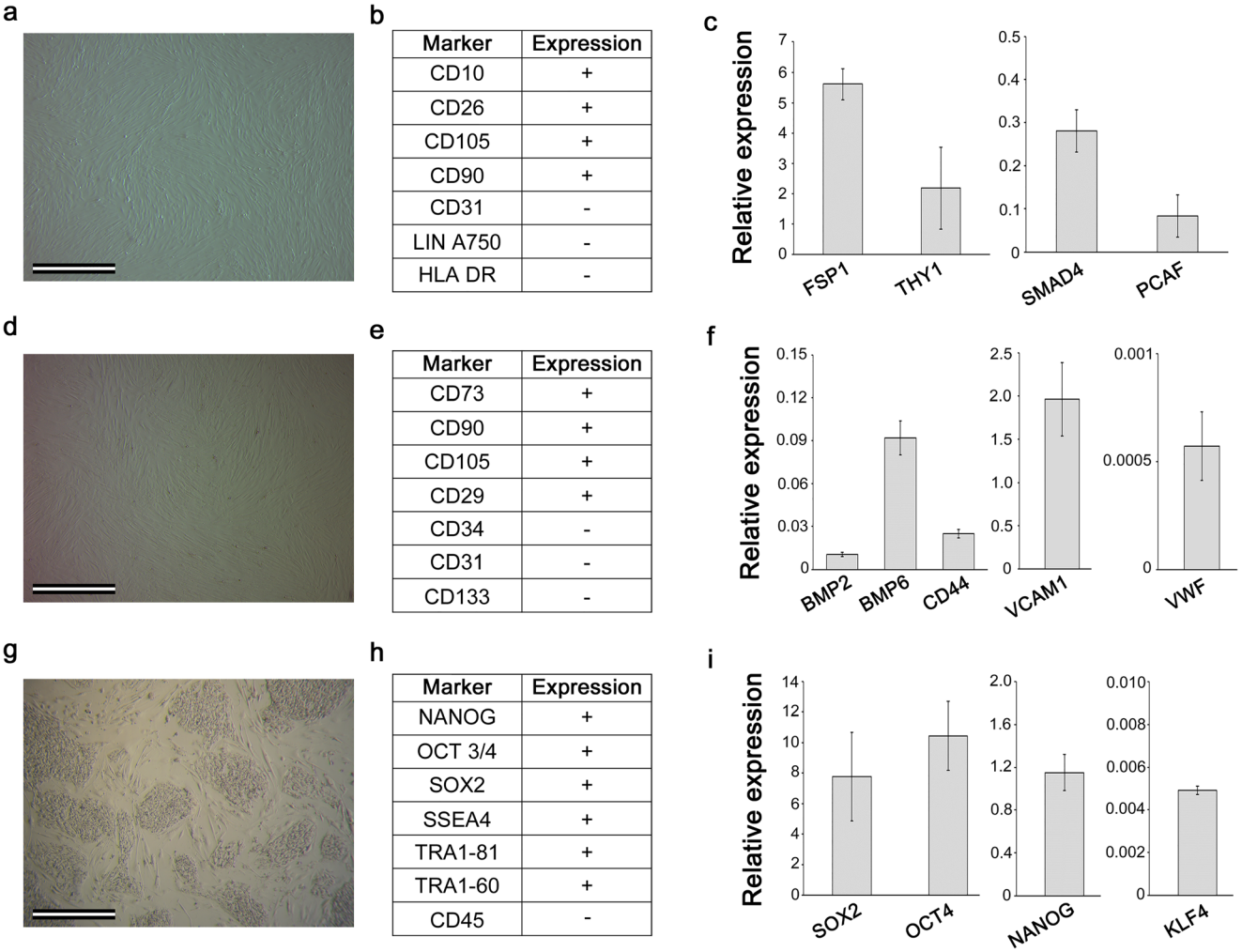

Marker	Expression
CD10	+
CD26	+
CD105	+
CD90	+
CD31	-
LIN A750	-
HLA DR	-

Marker	Expression
CD73	+
CD90	+
CD105	+
CD29	+
CD34	-
CD31	-
CD133	-

Marker	Expression
NANOG	+
OCT 3/4	+
SOX2	+
SSEA4	+
TRA1-81	+
TRA1-60	+
CD45	-

Fig. 2 Characterization of the cultured cells. hDFs: **(a)** Representative phase-contrast micrograph of hDFs (passage 7, day 7). **(b)** FACS analysis of hDFs. **(c)** RT-PCR findings of hDFs. hBM-MSCs: **(d)** Phase-contrast micrograph showing characteristic fibroblastoid morphology of hBM-MSCs (Passage 2, day 7). **(e)** FACS analysis of hBM-MSCs. **(f)** RT-PCR findings of hBM-MSCs. hiPSCs: **(g)** Phase-contrast image of hiPSCs on the VTN-coated surface proliferating in colony form unlike other cells (passage 21, day 5). **(h)** FACS analysis of hiPSCs. **(i)** RT-PCR findings of the cultured hiPSCs. All experiments were performed in triplicate. Errors bars: s.d ($n = 3$). Scale bars: **(a, d, g)** 100 μm. (FSP1: Fibroblast-specific protein 1; THY1: Cluster of Differentiation 90; SMAD4: SMAD Family Member 4; PCAF: Lysine Acetyltransferase 2B; BMP2: Bone morphogenetic protein 2; BMP6: Bone morphogenetic protein 6; CD44: Hematopoietic Cell E- and L-Selectin Ligand; VCAM1: Vascular Cell Adhesion Molecule 1; VWF: Von Willebrand Factor; SOX2: Sex determining region Y (SRY)-box 2; OCT4: Octamer-binding transcription factor 4; NANOG: Homeobox transcription factor Nanog; KLF4: Kruppel-like factor 4)

eosin (H&E) staining performed to examine the efficacy of the decellularization protocols (i.e. evaluation of cell nuclei and ECM distribution). For all three cell culture types, the light micrographs showed that while the cell nuclei were prominent in the ECMs before decellularization, they were removed from the culture at varying levels after decellularization, and the ECMs were substantially preserved. Among the studied protocols, Protocol 3 was found to be more effective than Protocols 1 and 2 in terms of eliminating a significant amount of cell nuclei from the culture while retaining ECM integrity (Fig. 3a). Scanning electron microscopy (SEM) findings showed that the integrity of the ECMs was retained and the characteristic cell morphologies were impaired on the culture plate surface for all three cell types (Fig. 3b). H&E stainings revealed that the hDF cell nucleus-like structures could still be found after Protocols 1 and 2, while they were not identified after Protocol 3. The SEM findings for hBM-MSCs-based ECM retrieval were also similar for hDFs, while hiPSC-based ECMs showed the effective removal of cells with Protocol 2 as well as Protocol 3, consistent with H&E histochemistry (Fig. 3b). Phase-contrast microscopy evaluations for all the three types of decellularized cell cultures were in line with the SEM findings (supplementary Fig. 4).

DNA and sGAG Content Measurements

DNA could be largely removed from cell cultures. The DNA content analyses revealed a value of 42.17 ± 6.29 ng/ECM for

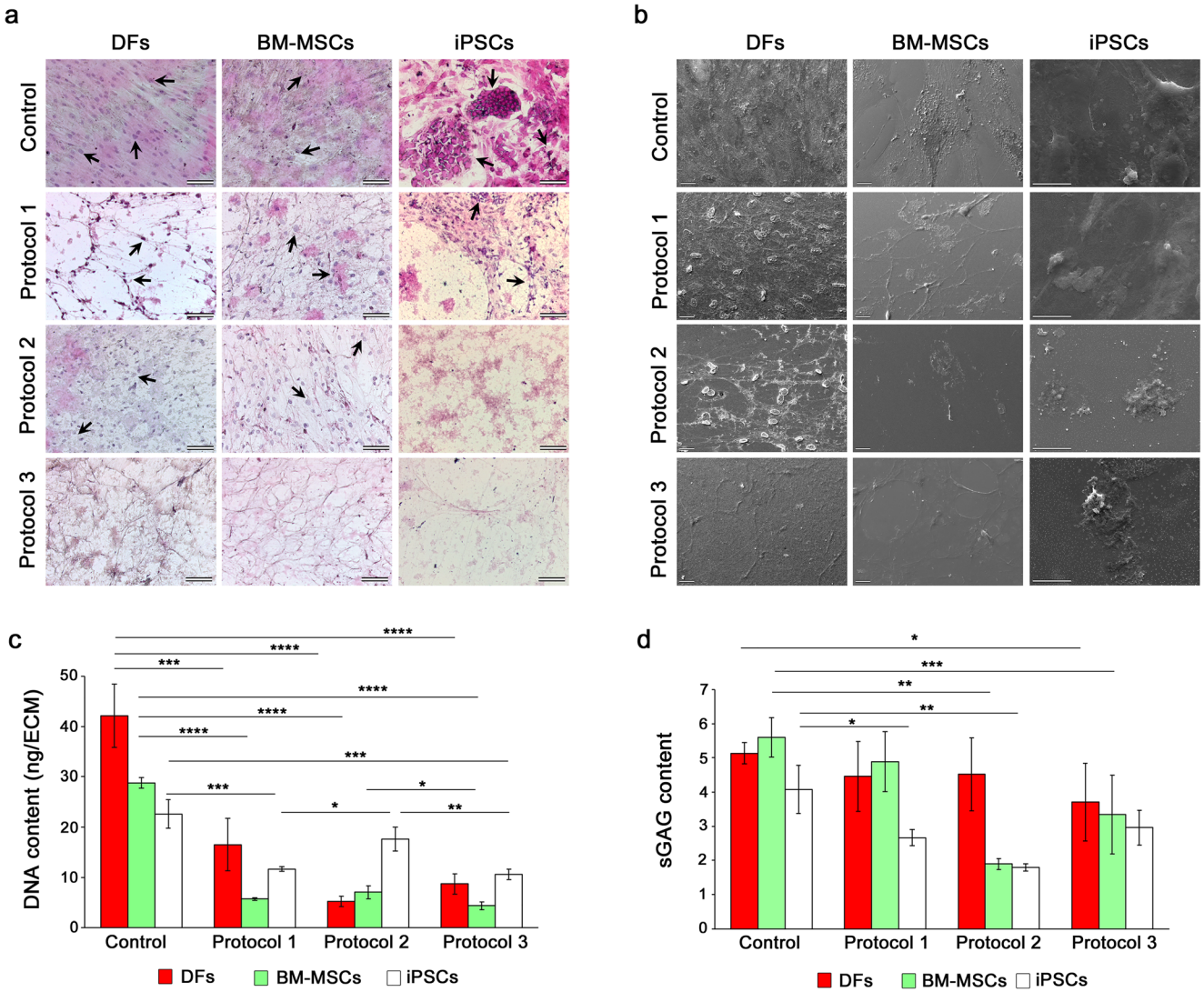

Fig. 3 Efficiency evaluation of decellularization protocols on human cells with different potencies. **(a)** Cell nuclei and ECM distribution of cell culture-derived ECMs after the application of different decellularization protocols (H&E stainings). Black arrows indicate the cell nucleus. There is no visible nucleus in Protocol 3-treated cell culture groups (Control is un-treated cell culture) (Scale bars: 100 μm). **(b)** SEM images of standard cell culture (Control) and decellularized cell culture-derived ECMs (Scale bars: 20 μm). **(c)** DNA, and **(d)** sGAG contents of the native and decellularized cell culture-derived ECMs following the application of different protocols. Error bars represent s.d. (n = 3) (* $p < 0.05$, ** $p < 0.01$, *** $p < 0.001$, **** $p < 0.0001$)

hDFs (1.0×10^6 cells) in the control group. The reductions in the DNA content were calculated from the ECMs obtained from each culture of 1.0×10^6 cells. After decellularization, the amount of DNA decreased significantly by 16.50 ± 5.22 ng/ECM ($p < 0.001$) in hDFs-based-ECMs using Protocol 1. On the other hand, the DNA amount in hDFs-based ECMs effectively decreased compared to the control after Protocol 2 by 5.17 ± 1.04 ng/ECM and after Protocol 3 by 8.67 ± 2.02 ng/ECM ($p < 0.0001$) (Fig. 3c). The DNA content analysis with hBM-MSCs also showed that the DNA, identified as 28.83 ± 1.04 ng/ECM in controls, was eliminated at a similar level after the decellularization protocols ($p < 0.0001$). When the efficacy of the protocols was compared, Protocol 3 was found to lead to a marked decrease of DNA of 4.33 ± 0.76 ng/ECM in hBM-MSCs-based ECMs ($p < 0.05$). hiPSCs studies have revealed a protocol efficacy similar to that observed in hBM-MSCs-based ECM studies, with Protocols 1 and 3 leading to significantly decreased DNA amounts (11.65 ± 0.51–10.57 ± 1.02) ($p < 0.001$) (Fig. 3c).

The sGAG content in ECMs was also measured to evaluate the decellularization efficacy. Aside from collagen, sGAGs are among the main components of ECM, providing a micro-environment convenient for the maintenance of basic cellular activities such as cell adhesion, migration and differentiation, and should therefore be protected in target tissue or cell culture-based ECMs after decellularization [22]. The sGAG amounts determined spectrophotometrically for the control cultures of hDFs, hBM-MSCs and hiPSCs were 5.13 ±

0.31 μg/ECM, 5.59 ± 0.57 μg/ECM and 4.07 ± 0.70 μg/ECM, respectively (Fig. 3d). Comparative analyses showed that the hDFs-based decellularized ECMs had higher sGAG contents in Protocol 2 and 3. The greatest difference was achieved with Protocol 3, with an sGAG level of 3.70 ± 1.13 μg/ECM ($p < 0.05$). In hBM-MSCs, a significant sGAG loss was observed in ECMs decellularized with Protocol 2 (1.89 ± 0.16 μg/ECM) ($p < 0.01$), while in hiPSC studies, no significant loss was observed when compared to the controls after the implementation of Protocol 3 (2.95 ± 0.51 μg/ECM), whereas a marked sGAG loss was noted, particularly after Protocol 2 ($p < 0.01$) (Fig. 3d).

Evalulation of Protein Distribution in Cell-Culture Based ECMs

Decellularized cultures differentially possessed significant ECM proteins. The ECM surrounding the cells contain cell adhesion proteins such as fibronectin and laminin, in addition to structural proteins, mainly various types of collagens (collagen types 1 and 3) [23]. The presence of these proteins in ECMs obtained from the three different types of cell cultures after decellularization was examined through immunofluorescence. The control groups were found to have varying levels of these proteins. The expressions of fibronectin, Col1A, Col3A and Laminin in the control groups were significantly higher in hiPSCs than that in the hBM-MSCs and hDFs (Fig. 4a). Col1A and FN were similarly higher than Laminin and Col3A, in the control cultures of hBM-MSCs and hDFs. Immunofluorescence micrographs showed that while FN and Col1 proteins were preserved to some extent after decellularization (Protocol 3) in hBM-MSCs- and hDFs-based ECMs, Laminin and Col3A were found significantly reduced. In hiPSCs, on the other hand, all of the above proteins were highly preserved when compared to other cell-based ECMs after decellularization (Fig. 4a). Protocol 3 was selected for the subsequent decellularization studies, since this protocol was found to be the most appropriate method among others.

Growth Factor Contents

Decellularized cultures possessed different levels of VEGF, TGFβ1 and PDGF. In addition to ECM proteins, several growth factors in natural ECMs exist in the membrane proteins bound to GAG chains which can adhere specifically to certain proteins. Growth factors such as VEGF, TGFβ1 and PDGF, normally known to exist in ECM, are involved in the regulation of cell migration, proliferation and differentiation through mutual interactions [3, 12]. ELISA findings indicated that PDGF concentrations in the control culture groups were 194.26 ± 56.14 pg/ECM, 164.20 ± 31.98 pg/ECM and 74.25 ± 4.98 pg/ECM in hDFs, hBM-MSCs and hiPSCs, respectively. After decellularization using Protocol 3, maximum levels of PDGF were measured in hBM-MSCs-based ECMs (65.65 ± 9.34 pg/ECM) compared to the other cells, and the greatest loss was noted in iPSCs-based decellularized ECM (Fig. 4b).

For the TGFβ1, the maximum level was found in the untreated hDF culture, while the lowest TGFβ1 level was 2155.63 ± 234.50 pg/ECM, noted in hiPSCs. Unlike in the control group, the maximum TGFβ1 amount preserved after decellularization was 1616.72 ± 87.93 pg/ECM, noted in decellularized hBM-MSCs-based ECM (Fig. 4c). The other growth factor measured in this study, VEGF, reached the highest level in hBM-MSCs by 90.13 ± 25.70 pg/ECM, when compared to the other cell types in the control groups. In line with these results, the highest level after decellularization was also noted in the hBM-MSCs-based decellularized ECM (35.01 ± 16.45 pg/ECM) (Fig. 4d).

Effects of Decellularized ECMs on hDF Proliferation

Decellularized cell cultures supported hDF proliferation in vitro. Figure 5 summarizes the findings of the spectrophotometric MTT assay and SEM analysis, in which the aim was to identify the proliferation behavior of hDFs on surfaces containing decellularized ECMs derived from different cell types with distinct potencies. No significant difference in the proliferation of hDFs was noted on the first day of culture (Fig. 5a). On day 3, proliferation of hDFs increased significantly on the hBM-MSCs-based ECM when compared to the control culture, on the other hand there was no significant difference between the proliferation capacities of the hDFs on hDF-based and hiPSC-based ECMs. On day 7, the cells maintained their viability and continued to proliferate accordingly (Fig. 5a, supplementary Fig. 5). The SEM analyses were in line with the spectrophotometric measurements. The cells gradually proliferated, and reached maximum levels by day 7, with the increase in proliferation capacity of hDFs being particularly remarkable on hBM-MSCs-based ECM (Fig. 5b).

Evaluation of Gene Expression Changes of hDFs on Decellularized Cell-Culture ECMs

Decellularized cell culture ECMs act as hDF differentiation inducers. Following the proliferation of hDFs on the three different decellularized cell-based ECMs, RT-PCR analyses were carried out to evaluate any potential changes in the expression of 14 different genes (including somatic, multipotent and pluripotent lineage specific genes), as part of an evaluation of the three different levels of potency. For this purpose, SOX2, OCT4, NANOG, KLF4, CD90, SMAD4, PCAF, FSP1, BMP-2, BMP-6, CD44, VCAM, COL1A1 and vWF genes were chosen. The gene expression levels of hDFs varied after culturing on different cell-based ECMs. In particular, a marked

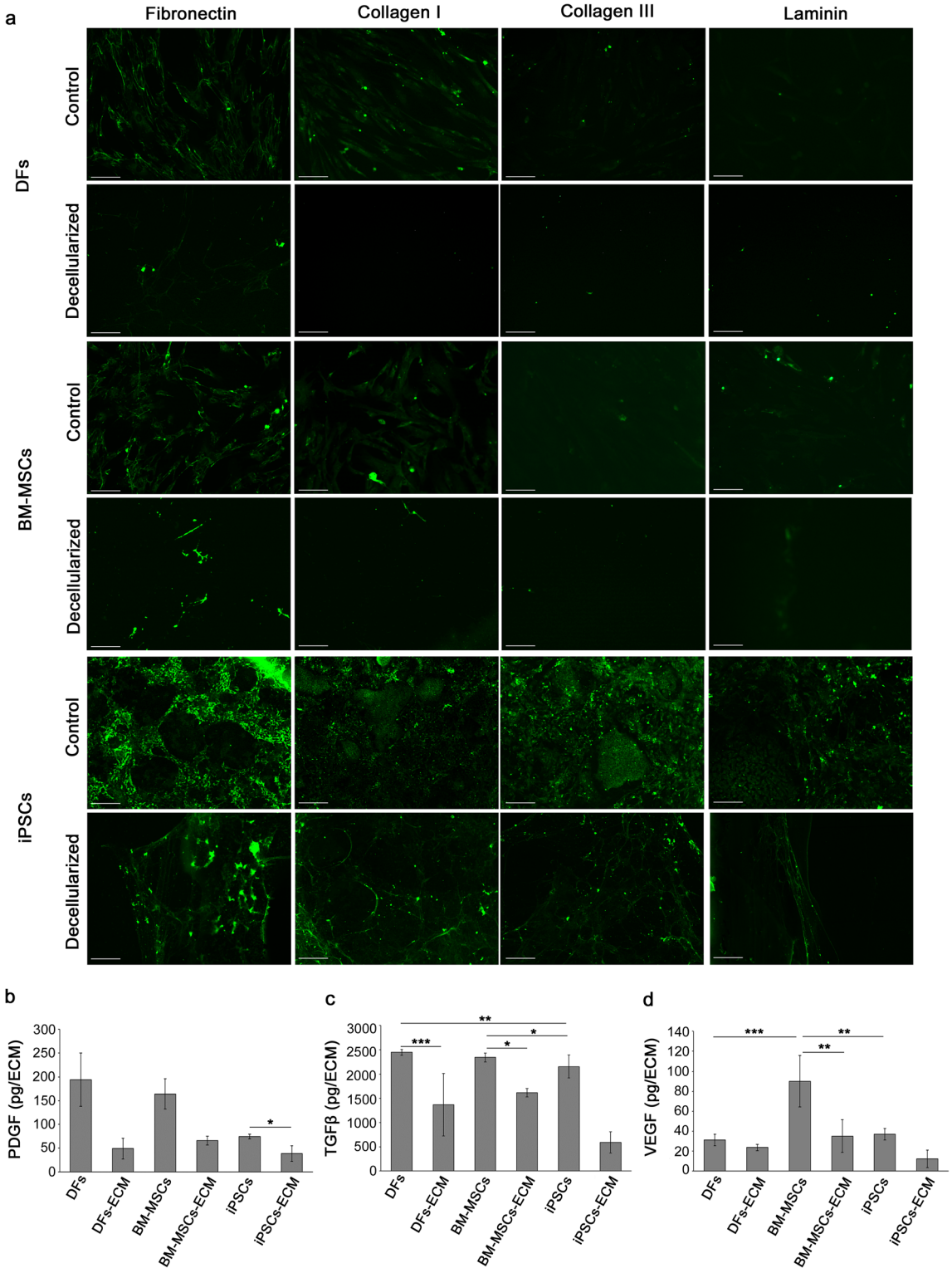

Fig. 4 Immunofluorescence microscopy and growth factor contents. **(a)** Fluorescence micrographs of Fibronectin, Laminin, Collagen Type I and III stainings of standard and decellularized (Protocol 3) cell cultures of hDFs, hBM-MSCs and hiPSCs (Scale bars: 200 μm). **(b-d)** ELISA findings evaluating the effect of decellularization on growth factor content of cell-cultured derived ECMs: **(b)** PDGF, **(c)** TGFβ, and **(d)** VEGF contents of standard and decellularized ECMs. Error bars represent s.d. (n = 3) (*$p < 0.05$, **$p < 0.01$, ***$p < 0.001$)

increase in the expression of certain genes was noted in hDFs cultured on hDF-based decellularized ECM (which was not the case for hBM-MSC- and hiPSC-based ECMs) compared to control hDFs (Fig. 6). The RT-PCR results, showing the changes in gene expression levels after hDFs' culture on hBM-MSC-based ECM, revealed significant increases in expressions of the

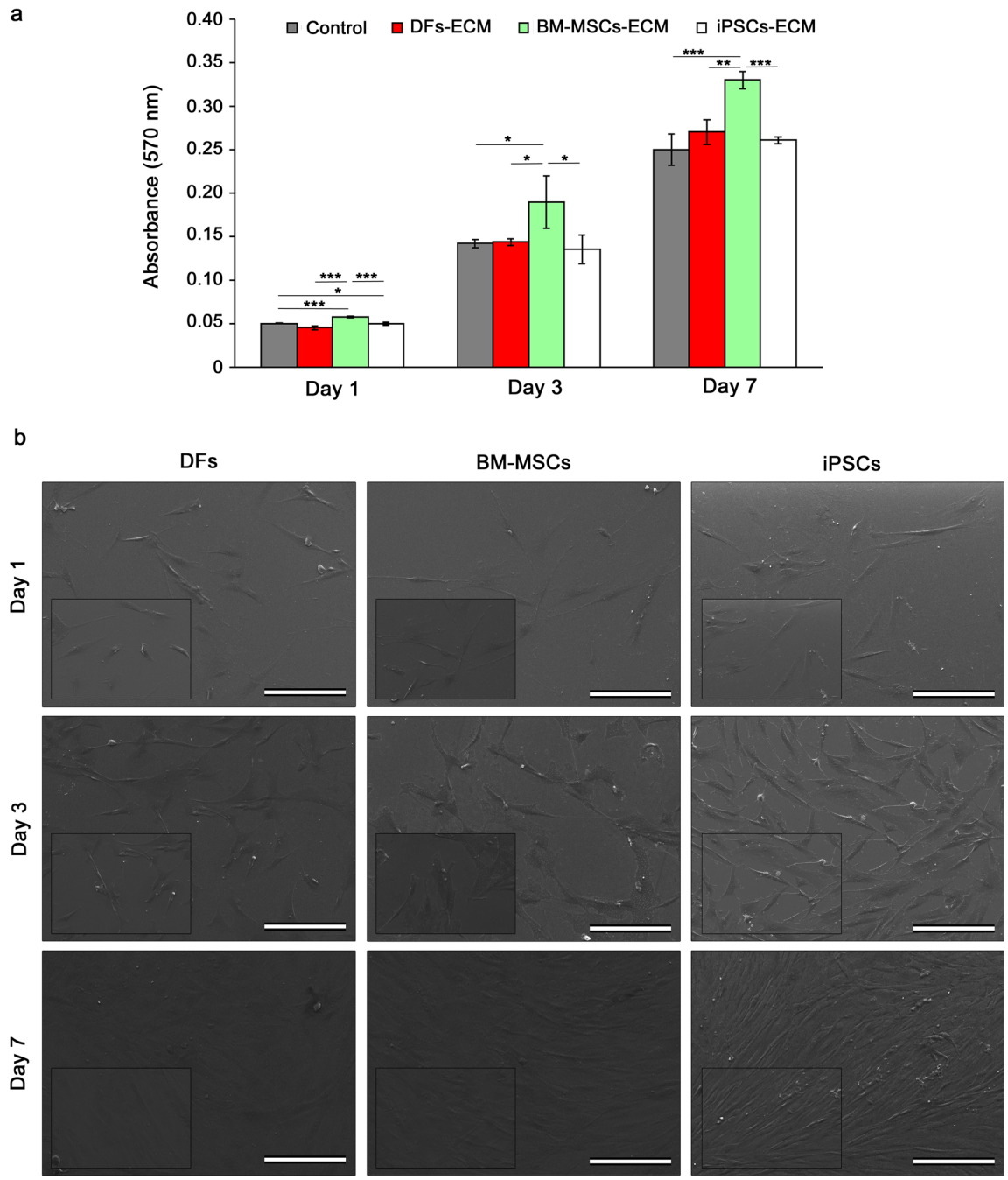

Fig. 5 Proliferation of hDFs on different cell culture-based ECMs. **(a)** In vitro MTT assay results of hDFs at day 1, 3 and 7 of the culture. **(b)** Representative SEM images demonstrating the surface distribution of hDFs on different decellularized ECM types at day 1, 3 and 7 of the culture. Error bars represent s.d. (n = 3) (* $p < 0.05$, ** $p < 0.01$, *** $p < 0.001$)

COL1A1 ($p < 0.0001$), SMAD4 ($p < 0.0001$), THY1 ($p < 0.01$), PCAF ($p < 0.001$), CD44 ($p < 0.01$) and CD106 ($p < 0.01$) genes when compared to the control group. Different from the control group and the other cell-based ECMs, hDF culture on hiPSC-based decellularized ECM showed significant increases in expression levels of the BMP6 ($p < 0.001$), FSP1 ($p < 0.01$), SMAD4 ($p < 0.01$) and KLF4 ($p < 0.01$) genes. Aside from these genes demonstrating significant increases in expression levels, no marked increases were noted in the expression of the vWF or NANOG genes, when compared to the controls (Fig. 6).

Discussion

This study has optimized the decellularization protocol for the isolation of the ECM from cells with different potencies, namely hDFs, hBM-MSCs and hiPSCs, and has also made a

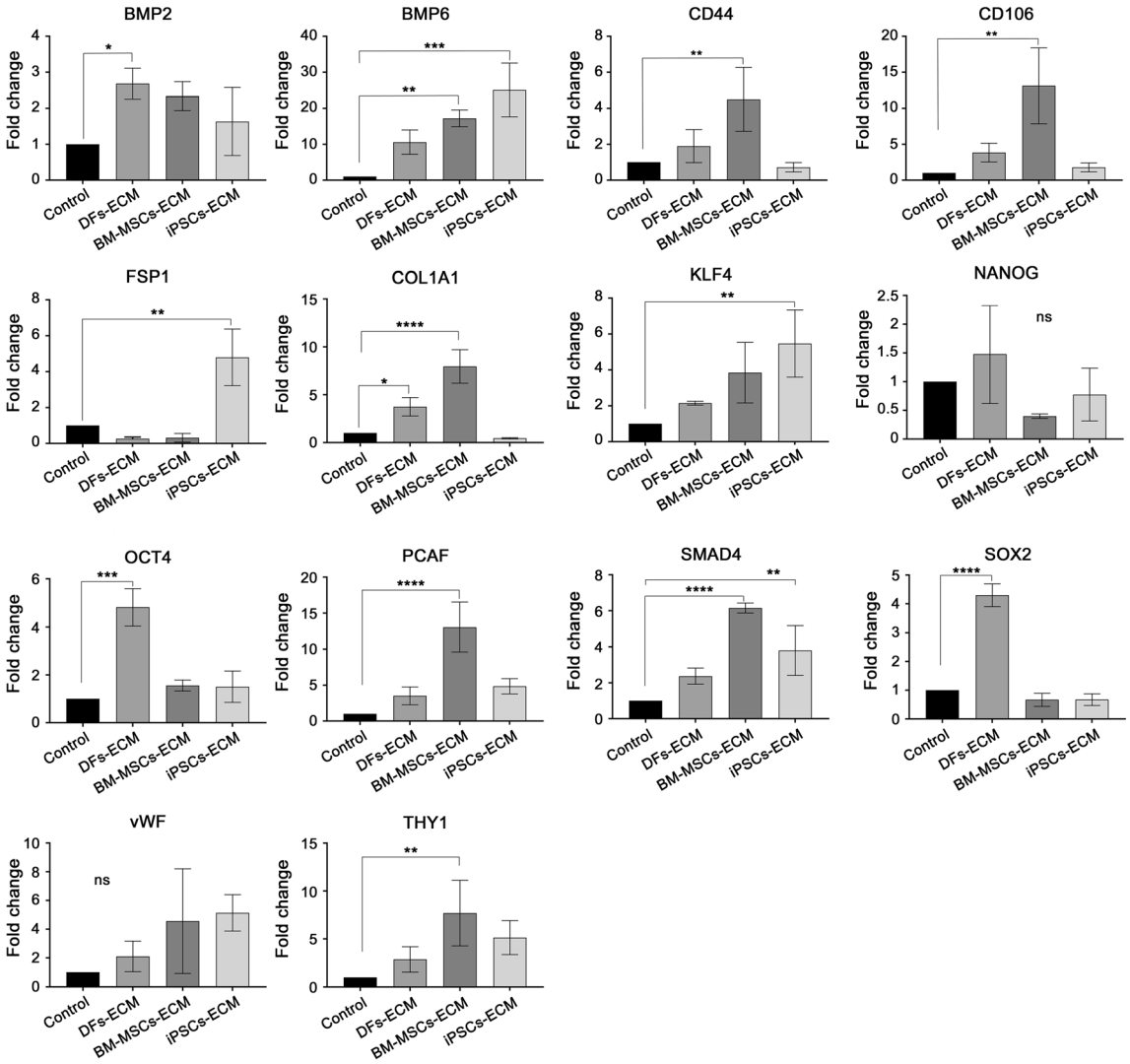

Fig. 6 Identification of gene expression changes. Real Time-PCR results of 14 selected genes, including somatic, multipotent and pluripotent lineage specific genes in hDFs cultured on different types of cell culture-based ECMs. Error bars represent s.d. (n = 3) (* $p < 0.05$, ** $p < 0.01$, *** $p < 0.001$, **** $p < 0.0001$)

comparative characterization of the ECMs isolated from these cell types. An evaluation of the efficacy of the examined decellularization protocols revealed that the quantities of ECM constituents, such as growth factors, sGAGs and ECM proteins, varied considerably between the different cell types. Moreover, this was the first study to assess hiPSC-derived ECMs maintained in a 2D culture, hence constituting a comprehensive evaluation of decellularization technologies for the tissue engineering of natural ECMs in cells that have not yet been exposed to any kind of induction/differentiation medium.

This study has also identified the potential changes in cellular properties (viability, proliferation, etc.) and the differentiation/gene expression of fully-differentiated hDFs on ECMs obtained from cell cultures with different levels of potency. Data collected in this study highlights the potential to mimic tissue/organ ECMs in cell remodeling, differentiation and advanced tissue engineering studies, as well as the use of ECMs obtained from unlimited natural cell sources.

In the first part of the study, the optimal decellularization protocols for each type of human cell cultures with different potencies were determined. Even though the primary aim of the decellularization process is to completely eliminate any cellular components and DNA from tissues, organs, and – most recently – cell cultures, it is important to minimize any loss of the ECM components during this process [3, 4]. Previous studies of tissue and organ decellularization procedures have mostly used a multi-step protocol approach involving physical, chemical and enzymatic processes [7, 16]. Despite the fact that their efficacy in tissue and organ-based studies has been controversial, some cell culture-based studies have reported that detergents such as Triton X-100, and alkaline reactives like ammonium hydroxide (NH_4OH) were more effective than enzymatic methods in the removal of cellular

components [5]. It has also been reported that the use of detergents with milder effects on organs/tissues, such as Triton X-100, in cell cultures allowed for the elimination of cellular materials without damaging the ECM constituents, such as sulfated glycosaminoglycans, growth factors and collagen. In addition to alkaline and mild detergents, the use of DNase and RNase solutions in the final stage was also proven to be effective in the elimination of DNA and RNA in different tissue and cell types [15, 24].

Previous studies using hBM-MSCs and hDFs have mostly employed an inducing growth medium containing ascorbic acid to enhance the ECM deposition. This indicates that the collection of the natural ECMs cannot be achieved by appropriately preserving the cellular characteristics. Besides, the hiPSCs have not been evaluated in a decellularization or ECM isolation study before. The present study established an optimal decellularization protocol that can be used for all three cell types. Depending on the findings of the efficacy analyses, the most suitable protocol which is common for hDFs, hBM-MSCs and hiPSCs is based on a 1% Triton X-100 and 20 mM NH_4OH solution [11].

In order to evaluate the efficacy of decellularization, the effects of ECM on cells and sGAG content were also investigated [22], and the results indicated that the optimized protocol ensured a high level of sGAG preservation in ECMs obtained from all three cell types. When each group was evaluated individually, the multipotent hBM-MSCs had a high amount of sGAG, originating from their own natural ECM, whereas pluripotent hiPSCs, which could be considered as being at the early stages of development, had minimum sGAG content, as expected.

The microenvironment surrounding the cells is known to be the main factor directing the properties, including the differentiation of cultured cells, possibly through receptor-ligand interactions. Clarifying of such effects depends on a complete understanding of cell-ECM interactions [24, 25]. While several factors are known to play roles in receptor-ligand interactions in the aforementioned natural cell microenvironments, matrix proteins, as the main components, play significant roles in such biological processes as protein synthesis, signal transduction, cell motility and cell division [26]. In addition to taking on the task as a physical substrate for cells, ECM also contains several collagen types and structural proteins as elastin, as well as cell adhesion proteins like fibronectin, laminin and vitronectin [14].

In the present study, the levels of fibronectin, an ECM protein that plays a key role in cell adhesion, were measured in decellularized ECMs. Among the cell types, somatic hDFs were found to have the highest level of fibronectin [19, 27, 28]. In contrast, pluripotent hiPSCs had markedly lower levels of fibronectin when compared to the other cells [29]. hiPSCs demonstrate relatively lower levels of ECM deposition than other cell types, as they proliferate in colonies. As expected, analyses of type 1 and type 3 collagen proteins, as the other predominant matrix proteins that play key roles in cell proliferation and differentiation, have indicated that their levels are higher in control cell cultures [14, 23].

One particular notable difference detected in this study was related to hiPSCs. Different to the fibroblastoid cell proliferation, ECM deposition in hiPSCs proliferating as colonies, was denser inside the colonies than through the periphery. It is therefore obvious that the difference in COL1A and COL3A quantities were attributable to colony deposition [30].

In this study, we also investigated the levels of laminin, being a protein with an RGD pattern that modulates cellular functions and provides structural support. In line with some other studies, laminin levels were found to have decreased in all cells with different potencies [31, 32]. Laminin, which was already low in the control group, decreased even further in ECM after decellularization, and could only be detected at very low levels in some regions of the 2D culture surface. On the other hand, a significant amount of laminin expression was noted in iPSCs, which has not yet been investigated in decellularization studies. Indeed, it is known that laminin proteins are expressed predominantly in the initial stages of development. While some decellularization studies report that laminin may be preserved in hDFs and hBM-MSCs-based-ECMs, those studies required additional procedures and cross-linking protocols to enhance ECM deposition [14, 33, 34].

As known, the natural microenvironment of cells includes various growth factors, ECM bound to GAG chains, and membrane proteins, aside from matrix proteins. It is known that growth factors are bound to particular proteins [14, 35]. Growth factors such as bFGF, VEGF, TGFβ1 and PDGF, which are known to bind to ECM under physiological conditions, can enhance cell migration, proliferation and differentiation through mutual interactions [3, 12].

In the present study we investigated certain levels of VEGF, TGFβ1 and PDGF in decellularized ECM, all of which are known to have significant effects on cell behavior. Based on previous reports, we expected to find elevated PDGF and TGFβ1 levels in somatic and multipotent cells, and it was remarkable to find that VEGF had markedly increased in multipotent hBM-MSCs when compared to the other groups [12, 36, 37]. On the other hand, the levels of VEGF, PDGF and TGFβ1 were much lower in hiPSCs that were addressed previously in this study. The ECM of pluripotent cells that are in the differentiation stage and carrying growth factor receptors is believed to bear growth factors at levels that permit their proliferation without differentiating [38]. These results appear to be congruent with previous studies. Moreover, the spectroscopic sGAG, IF staining findings and growth factor analyses of the decellularized cell culture ECMs investigated in this study are, on the whole, consistent with one other, and suggest that growth factors essentially

exist as bound to sGAGs and ECM proteins. The enzymes found in ECMs, such as matrix metalloproteases (MMPs), collagenases and stromelysin, are known to release growth factors by degrading the sGAG molecules that are bound to these factors [10, 39].

Studies with cell-based ECMs have mostly investigated the properties of multipotent cells that can differentiate between the different types of ECM after being re-seeded on ECMs. On the other hand, the effects on differentiated cells such as hDFs or cells with low potential for differentiation have been evaluated in only a number of studies. The present study addressed whether the different potencies of ECM constituents are able to direct hDFs away from their innate microenvironment and enable them to differentiate into different cell types or adapt to new microenvironments.

Findings indicated that hDFs exhibited higher levels of viability and proliferation on multipotent ECMs than on other types of ECMs. The ECM matrix proteins and sGAG contents were not markedly different between the decellularized ECMs, hence the differential effects may be attributable to the greater level of preservation of growth factors in multipotent ECM, and to the synergistic effects of the combinations of the aforementioned active constituents [6, 12, 13, 40–42].

In addition, the expression of a significant proportion of the investigated genes (BMP2, CD44, CD106, COL1, PCAF, SMAD4, KLF4) had significantly increased under the influence of multipotent decellularized ECM (hBM-MSCs), however some unexpected results were also observed. For example, it was expected that the SOX2 and OCT4 genes would modulate the multipotent and pluripotent effect of ECMs; however, they displayed limited increases in the decellularized microenvironments of hDFs. On the other hand, the pluripotent microenvironment was found to modulate the FSP1, BMP6 and KLF4 genes, in contrast to other decellularized ECMs.

In order to identify the basis behind such changes in the gene expressions of somatic hDFs, their biology needs to be evaluated. Previous studies have shown that hDFs have some features resembling the multipotent cells; clonal analyses have suggested that these cells form a heterogeneous population containing precursor cells. Indeed, microarray-based gene expression analyses have reported that genes expressed by hBM-MSCs were also expressed by hDFs to a substantial level, while some other studies have indicated the multipotent differentiation potential of these cells have actually provided evidence that they could differentiate into neuronal and mesodermal lineages [43–45]. Studies also suggest that, hDFs may differentiate into adipocyte-, chondrocyte- and osteoblast-like cells under the appropriate conditions. Hence, our study suggests that different types and compositions of decellularized ECMs may have influenced the hDFs. It is not easy to attribute changes in gene expression to a single factor, although the synergistic effects of the aforementioned decellularized ECM components may have played potential roles.

It could be asserted that the changes in gene expressions have resulted both from the growth factors and sGAG contents of the cell culture ECMs. BMPs are osteoblastic markers also known to play significant roles in vascular endothelial cells and angiogenesis [46]. Studies with hDFs have reported that although fibroblasts do not typically express osteoblastic markers, they may express significant levels of BMP2 or BMP7 when exposed to osteogenic induction [47]. It is also known that the presence of TGF-β1 contributes to the protection and development of bone tissue by enhancing the synthesis of the proteoglycan matrix and collagen; TGF-β1 is also expressed by hDFs under in-vitro osteogenic differentiation [48]. TGF-β1 is also involved in the increase in CD44 expression. Fibroblasts transform into myofibroblasts during the natural wound healing process, enabling effective healing, and is mainly regulated by TGFβ1 [49]. Similarly, the SMAD4 gene also expresses a signal transduction protein activated by the transmembrane serine-treonin receptor kinases that is responsible for TGF-β1 signaling. It is possible to interpret that different TGF-β1 concentrations detected in decellularized ECMs may bring about increases in the expression of BMP2, BMP6, CD44 and SMAD4 genes, in addition to other combinations. The characteristics noted for each gene and the differentiation potential of hDFs may indicate that these cells are perhaps directed towards the osteogenic and/or endothelial lineages, although the effect may be attributed to the fact that the VEGF and TGF-β1 detected in the ECM-based structures was in different combinations. Another growth factor identified in decellularized cultures is PDGF, which is known to be involved in cell proliferation and migration. Its contribution to osteogenic differentiation is not known [50]; additionally the mechanism through which PDGF regulates cell differentiation is still unknown [51].

Another point that is worthy of note in other gene expression variations is that hDFs showed significant elevations in pluripotent OCT4, SOX2, KLF4 and NANOG gene levels when cultured on somatic hDF-based ECMs. Previous studies also report that hDFs express high levels of KLF4, a gene known to be expressed by pluripotent stem cells [19, 52, 53]. It has also been reported that hDFs express a certain level of stem cell transcription factors, and that some of these genes such as OCT4, are expressed by pluripotent cells. Reprogramming studies have indicated that environmental factors may affect the expression of stem cell-specific genes in somatic hDFs, such as the use of growth factors like FGF, culture conditions and low oxygen levels. While environmental effects are known to enhance the translation of such genes as OCT4, SOX2 and NANOG, hDFs have been reported to

survive longer in cultures under similar environmental conditions [54, 55].

Studies investigating MSCs have shown that factors such as TGFB1, PDGF and FGF play key roles in the signaling processes, and MSCs can therefore differentiate into different lineages. Nonetheless, considering the fact that the differentiation characteristics of hDFs resemble those of MSCs, it may be due to a combination of such factors which direct hDFs to different cell types [56]. In addition to these genes, relative increases in the expression of the PCAF, VCAM-1 (CD106), vWF and Thy-1 (CD90) genes were also observed, particularly under the influence of hBM-MSCs-derived ECM. PCAF is known to play a role in differentiation processes, angiogenesis and cell cycle progression [57], while vWF is a glycoprotein that is produced by endothelial cells, and which is specific to these cells [58–60], and Thy-1 (CD90) and VCAM-1 (CD106) are also known to be expressed by endothelial cells [61–64]. Considering these findings altogether, it is possible that hDFs may have tendency to differentiate into the endothelial lineage when cultured in multipotent microenvironments [63]. Another important effect of the multipotent microenvironment on hDFs was observed in COL1, in line with earlier studies reporting that hBM-MSCs-based ECMs enhance the expression of chondrocyte-related genes, for reasons that are as yet unclear [44].

As a proof of concept, the present study has investigated the relationship between cells and microenvironment potency using state of the art decellularization approach. It has been shown that ECMs with significantly preserved natural bioactive components regulating cell differentiation can be obtained from unlimited sources of cell cultures. It is remarkable that cells undergo molecular changes in relation to the effects of the ECMs obtained from different cell types. Pluripotent ECMs should be investigated extensively in prospective studies, as their use with terminally-differentiated somatic cells or undifferentiated stem cells have the potential to provide as yet unpredictable results. It seems feasible to incorporate such decellularized microenvironments as biomimetic components into fabricated constructs for a variety of bioengineering applications. In addition, clarification of the potential synergistic effects of decellularized ECMs may contribute to in vitro drug development, as well as remodeling studies. Although challenges remain, the present study suggests that cell culture-based ECMs may perhaps be considered as an alternative approach for the direct differentiation of even somatic cells into other cell types in the future.

Funding Information This work was supported by The Scientific and Technological Research Council of Turkey, Ankara, Turkey (Grant No. 214 M159).

Compliance with Ethical Standards

Disclosure of Interest Y.M.E. is the founder and shareholder of Biovalda Health Technologies, Inc. (Ankara, Turkey). The authors have patent applications in relation to regenerative biomaterials. The authors declare no competing financial interests in relation to this particular article.

Consent for Publication This manuscript has been approved by all authors. The authors are alone responsible for the content and writing of the paper.

References

1. Langer, R., & Vacanti, J. (1993). Tissue engineering. *Science, 260*, 920–926.
2. Elcin, Y. M. (2003). *Tissue engineering, stem cells and gene therapies. AEMB series: 534*. NY & London: Kluwer-Plenum. isbn:0-306-47788-2.
3. Badylak, S. F., Freytes, D. O., & Gilbert, T. W. (2009). Extracellular matrix as a biological scaffold material: Structure and function. *Acta Biomaterialia, 5*, 1–13.
4. Badylak, S. F., Taylor, D., & Uygun, K. (2011). Whole-organ tissue engineering: Decellularization and recellularization of three-dimensional matrix scaffolds. *Annual Review of Biomedical Engineering, 13*, 27–53.
5. Parmaksiz, M., Elçin, A. E., & Elçin, Y. M. (2019). Decellularized bovine small intestinal submucosa-PCL/hydroxyapatite-based multilayer composite scaffold for hard tissue repair. *Materials Science and Engineering: C, 94*, 788–797.
6. Pati, F., Jang, J., Ha, D. H., et al. (2014). Printing three-dimensional tissue analogues with decellularized extracellular matrix bioink. *Nature Communications, 5*, 3935.
7. Parmaksiz, M., Elcin, A. E., & Elcin, Y. M. (2017). Decellularization of bovine small intestinal submucosa and its use for the healing of a critical-sized full-thickness skin defect, alone and in combination with stem cells, in a small rodent model. *Journal of Tissue Engineering and Regenerative Medicine, 11*, 1754–1765.
8. Wan, L., Chen, Y., Wang, Z., et al. (2017). Human heart valve-derived scaffold improves cardiac repair in a murine model of myocardial infarction. *Scientific Reports, 7*, 39988.
9. Simões, I. N., Vale, P., Soker, S., et al. (2017). Acellular urethra bioscaffold: Decellularization of whole urethras for tissue engineering applications. *Scientific Reports, 7*, 41934.
10. Cheng, C. W., Solorio, L. D., & Alsberg, E. (2014). Decellularized tissue and cell-derived extracellular matrices as scaffolds for orthopaedic tissue engineering. *Biotechnology Advances, 32*, 462–484.
11. Sart, S., Ma, T., & Li, Y. (2014). Extracellular matrices decellularized from embryonic stem cells maintained their structure and signaling specificity. *Tissue Engineering Part A, 20*, 54–66.
12. Xing, Q., Yates, K., Tahtinen, M., Shearier, E., Qian, Z., & Zhao, F. (2015). Decellularization of fibroblast cell sheets for natural extracellular matrix scaffold preparation. *Tissue Engineering*Part C, Methods*, 21*, 77–87.
13. Xu, Y., Xu, G. Y., Tang, C., et al. (2015). Preparation and characterization of bone marrow mesenchymal stem cell-derived extracellular matrix scaffolds. *Journal of Biomedical Materials Research Part B, 103*, 670–678.
14. Wei, W., Li, J., Chen, S., et al. (2017). In vitro osteogenic induction of bone marrow mesenchymal stem cells with a decellularized matrix derived from human adipose stem cells and in vivo

implantation for bone regeneration. *Journal of Materials Chemistry B, 5*, 2468–2482.
15. Zhang, W., Zhu, Y., Li, J., et al. (2016). Cell-derived extracellular matrix: Basic characteristics and current applications in orthopedic tissue engineering. *Tissue Engineering, Part B: Reviews, 22*, 193–207.
16. Parmaksiz, M., Dogan, A., Odabas, S., Elçin, A. E., & Elçin, Y. M. (2016). Clinical applications of decellularized extracellular matrices for tissue engineering and regenerative medicine. *Biomedical Materials, 11*, 22003.
17. Dzafic, E., Stimpfel, M., Novakovic, S., Cerkovnik, P., & Virant-Klun, I. (2014). Expression of mesenchymal stem cells-related genes and plasticity of aspirated follicular cells obtained from infertile women. *BioMed Research International, 2014*, 508216.
18. Kulterer, B., Friedl, G., Jandrositz, A., et al. (2007). Gene expression profiling of human mesenchymal stem cells derived from bone marrow during expansion and osteoblast differentiation. *BMC Genomics, 8*, 70–84.
19. Lorenz, K., Sicker, M., Schmelzer, E., Rupf, T., Salvetter, J., Schulz-Siegmund, M., & Bader, A. (2008). Multilineage differentiation potential of human dermal skin-derived fibroblasts. *Experimental Dermatology, 17*, 925–932.
20. Abujarour, R., Valamehr, B., Robinson, M., Rezner, B., Vranceanu, F., & Flynn, P. (2013). Optimized surface markers for the prospective isolation of high-quality hiPSCs using flow cytometry selection. *Scientific Reports, 3*, 1179.
21. Gilbert, T. W., Freund, J. M., & Badylak, S. F. (2009). Quantification of DNA in biologic scaffold materials. *The Journal of Surgical Research, 152*, 135–139.
22. Chen, X. D., Dusevich, V., Feng, J. Q., Manolagas, S. C., & Jilka, R. L. (2007). Extracellular matrix made by bone marrow cells facilitates expansion of marrow-derived mesenchymal progenitor cells and prevents their differentiation into osteoblasts. *Journal of Bone and Mineral Research, 22*, 1943–1956.
23. Mikami, T., & Kitagawa, H. (2017). Sulfated glycosaminoglycans: Their distinct roles in stem cell biology. *Glycoconjugate Journal, 34*, 725–735.
24. Guilak, F., Cohen, D. M., Estes, B. T., Gimble, J. M., Liedtke, W., & Chen, C. S. (2009). Control of stem cell fate by physical interactions with the extracellular matrix. *Cell Stem Cell, 5*, 17–26.
25. Uygun, B. E., Soto-Gutierrez, A., Yagi, H., Izamis, et al. (2010). Organ reengineering through development of a transplantable recellularized liver graft using decellularized liver matrix. *Nature Medicine, 16*, 814–820.
26. Nishio, K., & Inoue, A. (2005). Senescence-associated alterations of cytoskeleton: Extraordinary production of vimentin that anchors cytoplasmic p53 in senescent human fibroblasts. *Histochemistry and Cell Biology, 123*, 263–273.
27. Ruoslahti, E. (1984). Fibronectin in cell adhesion and invasion. *Cancer Metastasis Reviews, 3*, 43–51.
28. Kinsey, R., Williamson, M. R., Chaudhry, S., Mellody, K. T., McGovern, A., Takahashi, S., Shuttleworth, C. A., & Kielty, C. M. (2008). Fibrillin-1 microfibril deposition is dependent on fibronectin assembly. *Journal of Cell Science, 121*, 2696–2704.
29. Gattazzo, F., Urciuolo, A., & Bonaldo, P. (2014). Extracellular matrix: A dynamic microenvironment for stem cell niche. *Biochimica et Biophysica Acta, 1840*, 2506–2519.
30. Chen, Y., Zheng, Y. L., Qiu, D. B., Sun, Y. P., Kuang, S. J., Xu, Y., He, F., Gong, Y. H., & Zhang, Z. G. (2015). An extracellular matrix culture system for induced pluripotent stem cells derived from human dental pulp cells. *European Review for Medical and Pharmacological Sciences, 19*, 4035–4046.
31. McIntosh, L., & Walle, C.F. van der. (2011). Control of mammalian cell behaviour through mimicry of the extracellular matrix environment. On Biomimetics, Dr. Lilyana Pramatarova (Ed.), InTech.
32. Kumada, Y., & Zhang, S. (2010). Significant type I and type III collagen production from human periodontal ligament fibroblasts in 3D peptide scaffolds without extra growth factors. *PLoS One, 5*, e10305.
33. Köllmer, M., Keskar, V., Hauk, T. G., Collins, J. M., Russell, B., & Gemeinhart, R. A. (2012). Stem cell-derived extracellular matrix enables survival and multilineage differentiation within superporous hydrogels. *Biomacromolecules, 13*, 963–973.
34. Atyabi, S. M., Atoon, S., Irani, S., Khorasani, M. T., & Joupari, M. D. (2016). Fibroblast cell behavior study on chitosan/laminin scaffolds for tissue engineering. *Minerva Biotecnologica, 4*, 187–192.
35. Hynes, R. O. (2009). Extracellular matrix: Not just pretty fibrils. *Science, 326*, 1216–1219.
36. Kagiwada, H., Yashiki, T., Ohshima, A., Tadokoro, M., Nagaya, N., & Ohgushi, H. (2008). Human mesenchymal stem cells as a stable source of VEGF-producing cells. *Journal of Tissue Engineering and Regenerative Medicine, 2*, 184–189.
37. Prewitz, M. C., Seib, F. P., von Bonin, M., Friedrichs, J., Stißel, A., Niehage, C., Müller, K., Anastassiadis, K., Waskow, C., Hoflack, B., Bornhäuser, M., & Werner, C. (2013). Tightly anchored tissue-mimetic matrices as instructive stem cell microenvironments. *Nature Methods, 10*, 788–794.
38. Schuldiner, M., Yanuka, O., Itskovitz-Eldor, J., Melton, D. A., & Benvenisty, N. (2000). Effects of eight growth factors on the differentiation of cells derived from human embryonic stem cells. *Proceedings of the National Academy of Sciences of the United States of America, 97*, 11307–11312.
39. Li, L., Asteriou, T., Bernert, B., Heldin, C. H., & Heldin, P. (2007). Growth factor regulation of hyaluronan synthesis and degradation in human dermal fibroblasts: Importance of hyaluronan for the mitogenic response of PDGF-BB. *The Biochemical Journal, 404*, 327–336.
40. Yang, C., Lin, S., & Yu, H. (1997). Effect of growth factors on dermal fibroblast contraction in normal skin and hypertrophic scar. *Journal of Dermatological Science, 14*, 162–169.
41. Murillo, J., Wang, Y., Xu, X., Klebe, R. J., Chen, Z., Zardeneta, G., Pal, S., Mikhailova, M., & Steffensen, B. (2008). Advanced glycation of type I collagen and fibronectin modifies periodontal cell behavior. *Journal of Periodontology, 79*, 2190–2199.
42. Windmolders, S., Boeck, A. D., Koninckx, R., et al. (2014). Mesenchymal stem cell secreted platelet derived growth factor exerts a pro-migratory effect on resident cardiac atrial appendage stem cells. *Journal of Molecular and Cellular Cardiology, 66*, 177–188.
43. Junker, J. P., Sommar, P., Skog, M., Johnson, H., & Kratz, G. (2010). Adipogenic, chondrogenic and osteogenic differentiation of clonally derived human dermal fibroblasts. *Cells, Tissues, Organs, 191*, 105–118.
44. Toma, J. G., Akhavan, M., Fernandes, K. J., Barnabé-Heider, F., Sadikot, A., Kaplan, D. R., & Miller, F. D. (2001). Isolation of multipotent adult stem cells from the dermis of mammalian skin. *Nature Cell Biology, 3*, 778–784.
45. Bussmann, B. M., Reiche, S., Marí-Buyé, N., Castells-Sala, C., Meisel, H. J., & Semino, C. E. (2016). Chondrogenic potential of human dermal fibroblasts in a contractile, soft, self-assembling, peptide hydrogel. *Journal of Tissue Engineering and Regenerative Medicine, 10*, E54–E62.
46. Dyer, L. A., Pi, X., & Patterson, C. (2014). The role of BMPs in endothelial cell function and dysfunction. *Trends in Endocrinology and Metabolism, 25*, 472–480.
47. Hee, C. K., Jonikas, M. A., & Nicoll, S. B. (2006). Influence of three-dimensional scaffold on the expression of osteogenic differentiation markers by human dermal fibroblasts. *Biomaterials, 27*, 875–884.
48. Aloise, A. C., Pereira, M. D., Duailibi, S. E., Gragnani, A., & Ferreira, L. M. (2014). TGF-β1 on induced osteogenic

differentiation of human dermal fibroblast. *Acta Cirúrgica Brasileira, 29*(Suppl 1), 01–06.
49. Midgley, A. C., Rogers, M., Hallett, M. B., Clayton, A., Bowen, T., Phillips, A. O., & Steadman, R. (2013). Transforming growth factor-β1 (TGF-β1)-stimulated fibroblast to myofibroblast differentiation is mediated by hyaluronan (HA)-facilitated epidermal growth factor receptor (EGFR) and CD44 co-localization in lipid rafts. *The Journal of Biological Chemistry, 288*, 14824–14838.
50. Kumar, A., Salimath, B. P., Stark, G. B., & Finkenzeller, G. (2010). Platelet-derived growth factor receptor signaling is not involved in osteogenic differentiation of human mesenchymal stem cells. *Tissue Engineering*. Part A*, 16*, 983–993.
51. Li, A., Xia, X., Yeh, J., et al. (2014). PDGF-AA promotes osteogenic differentiation and migration of mesenchymal stem cell by down-regulating PDGFRα and derepressing BMP-Smad1/5/8 signaling. *PLoS One, 9*, e113785.
52. Alt, E., Yan, Y., Gehmert, S., Song, Y. H., Altman, A., Gehmert, S., Vykoukal, D., & Bai, X. (2011). Fibroblasts share mesenchymal phenotypes with stem cells, but lack their differentiation and colony-forming potential. *Biology of the Cell, 103*, 197–208.
53. Ulrich, C., Hart, M. L., Rolaufs, B., et al. (2012). Mesenchymal stromal cells and fibroblasts. *Journal of Tissue Science & Engineering, 3*, e109.
54. Zangrossi, S., Marabese, M., Broggini, M., Giordano, R., D'Erasmo, M., Montelatici, E., Intini, D., Neri, A., Pesce, M., Rebulla, P., & Lazzari, L. (2007). Oct-4 expression in adult human differentiated cells challenges its role as a pure stem cell marker. *Stem Cells, 25*, 1675–1680.
55. Page, R. L., Ambady, S., Holmes, W. F., Vilner, L., Kole, D., Kashpur, O., Huntress, V., Vojtic, I., Whitton, H., & Dominko, T. (2009). Induction of stem cell gene expression in adult human fibroblasts without transgenes. *Cloning and Stem Cells, 11*, 417–426.
56. Ng, F., Boucher, S., Koh, S., Sastry, K. S., Chase, L., Lakshmipathy, U., Choong, C., Yang, Z., Vemuri, M. C., Rao, M. S., & Tanavde, V. (2008). PDGF, TGF-, and FGF signaling is important for differentiation and growth of mesenchymal stem cells (MSCs): Transcriptional profiling can identify markers and signaling pathways important in differentiation of MSCs into adipogenic, chondrogenic, and osteogenic lineages. *Blood, 112*, 295–307.
57. Yamanaka, S., Yokote, S., Yamada, A., et al. (2014). Adipose tissue-derived mesenchymal stem cells in long-term dialysis patients display downregulation of PCAF expression and poor angiogenesis activation. *PLoS One, 9*, e102311.
58. Zanetta, L., Marcus, S. G., Vasile, J., Dobryansky, M., Cohen, H., Eng, K., Shamamian, P., & Mignatti, P. (2000). Expression of von Willebrand factor, an endothelial cell marker, is up-regulated by angiogenesis factors: A potential method for objective assessment of tumor angiogenesis. *International Journal of Cancer, 85*, 281–288.
59. Pusztaszeri, M. P., Seelentag, W., & Bosman, F. T. (2006). Immunohistochemical expression of endothelial markers CD31, CD34, von Willebrand factor, and Fli-1 in normal human tissues. *The Journal of Histochemistry and Cytochemistry, 54*, 385–395.
60. Blasi, A., Martino, C., Balducci, L., et al. (2011). Dermal fibroblasts display similar phenotypic and differentiation capacity to fat-derived mesenchymal stem cells, but differ in anti-inflammatory and angiogenic potential. *Vascular Cell, 3*, 5.
61. Schmidt, M., Gutknecht, D., Simon, J. C., Schulz, J. N., Eckes, B., Anderegg, U., & Saalbach, A. (2015). Controlling the balance of fibroblast proliferation and differentiation: Impact of Thy-1. *The Journal of Investigative Dermatology, 135*, 1893–1902.
62. Halfon, S., Abramov, N., Grinblat, B., & Ginis, I. (2011). Markers distinguishing mesenchymal stem cells from fibroblasts are down-regulated with passaging. *Stem Cells and Development, 20*, 53–66.
63. Lv, F. J., Tuan, R. S., Cheung, K. M., & Leung, V. Y. (2014). Concise review: The surface markers and identity of human mesenchymal stem cells. *Stem Cells, 32*, 1408–1419.
64. Velazquez, O. C., Snyder, R., Liu, Z. J., Fairman, R. M., & Herlyn, M. (2002). Fibroblast-dependent differentiation of human microvascular endothelial cells into capillary-like 3-dimensional networks. *The FASEB Journal, 16*, 1316–1318.